DIFFERENTIAL RADAR INTERFEROMETRY FOR MINE SUBSIDENCE MONITORING

Linlin Ge[1], Hsing-Chung Chang[1], Lijiong Qin[1], Ming-han Chen[1], and Chris Rizos[1]

[1]School of Surveying & Spatial Information Systems,
The University of New South Wales,
Sydney NSW 2052, AUSTRALIA

Abstract

The history of mining disasters includes cases of subsidence and collapse into workings, and also a number of inrushes into underground mines, where deficiencies in surveying, or in maintenance and interpretation of plans, were prime factors. The most recent incident in Australia was at the Gretley Colliery in NSW, in 1996. The most recent such incident in the USA was at the Quecreek Mine in Somerset County, in 2002. There is one thing common between the two incidents: the mining surface was too close to the abandoned workings and nobody knew it. Is it possible to prevent such mining disasters by monitoring subsidence as the signature of mining activity using differential radar interferometry (DInSAR)? In this paper, it is proposed to use GPS to assist precise georeference and ensure sub-centimetre accuracy of InSAR results and GIS to interpret, archive, and deliver the subsidence data derived from InSAR. The procedure is being tested in Appin, southwest of Sydney, Australia.

1. Introduction

The history of mining disasters includes cases of subsidence and collapse into workings, and also a number of inrushes into underground mines, where deficiencies in surveying, or in maintenance and interpretation of plans, were prime factors. The most recent incident in Australia was at the Gretley Colliery in NSW, in 1996. In that accident four men were engulfed by the water from long-abandoned old workings of the Young Wallsend Colliery, swept away and drowned. It was discovered that the mine was working to a plan that showed the Young Wallsend Colliery was located more than 100m away from the point of holing-in, while it was actually only 7 or 8 metres away. The most recent incident in the USA was at the Quecreek Mine in Somerset County, in 2002. In that accident 9 miners were trapped underground for 77 hours, in cold black water sometimes over their heads, although they were all rescued. It was found that the mine was working to a plan that showed the old mine was located more than 91m away from the point of holing-in, while it was actually right on top.

There is one thing common between the two incidents: the mining surface was too close to the abandoned workings and nobody knew it. Is it possible to prevent such mining disasters by monitoring subsidence as the signature of mining activity using differential radar interferometry (DInSAR)? In order for DInSAR to function as an early warning technique, the result should be: a) accurate (sub-centimetre accuracy), b) precisely georeferenced, c) well-archived, and d) readily available. Therefore, it is proposed to integrate InSAR with GPS and GIS to address this application.

Ground subsidence is the lowering or collapse of the land surface, and is caused by a number of natural and human-induced activities. Natural subsidence occurs when the ground collapses into underground cavities produced by the solution of limestone or other soluble materials by groundwater. Most current subsidence in the corridor is human induced, and is related to

underground mining. The rocks above mine workings may not have adequate support and can collapse from their own weight either during mining or long after mining is completed.

Factors effecting Subsidence include (Nesbitt, 2003):

- Depth of Cover,
- Overlying Strata Properties,
- Seam Thickness,
- Panel Width,
- Chain Pillar Size, and
- Surface Topography.

The need of subsidence monitoring in underground mining is multi-fold:

- Legislation,
- Subsidence Prediction,
- Maximise Coal Extraction,
- Structural Design,
- Risk Management, and
- Environmental Monitoring.

Therefore, ground subsidence due to underground mining is of major concern of the mining industry, government regulator, and environmental groups, to name only a few.

Subsidence is currently monitored by repeated ground survey using automatic/digital levels (in line levelling), total stations (in EDM height traversing) and GPS receivers (in static and real-time-kinematic (RTK) survey) (Schofield, 1993). Both digital level and total station can deliver 0.1mm height change resolution while GPS 5mm in static and 2-3cm in RTK.

On the other hand, the differential radar interferometry (D-InSAR) that will be presented in the following sections of this paper can deliver ~1cm height change resolution. Since radar beam scans in range direction, the movement of the platform in azimuth direction completes the 2D imaging of the mining region. The current geodetic technologies mentioned earlier, however, can only measure subsidence on a point-by-point basis. Therefore, D-InSAR and current geodetic technologies are complementary in monitoring ground subsidence due to underground mining.

2. Methodology

Synthetic Aperture Radar (SAR) measures distance information encoded in *phase*. Therefore, interferometric data can be obtained from two SAR images, and contains height information of a selected scene. The software application EarthView InSAR (EV-InSAR), a product of Atlantis (Atlantis, 2003), is used to generate digital elevation model (DEM) and height changes through the use of repeat-pass SAR interferometry (Atlantis, 2002).

Differential Interferometric Synthetic Aperture Radar (D-InSAR) is a radar technique to detect the surface deformations by computing a differential interferogram of the same scene over two repeat-pass acquisitions. There are various D-InSAR techniques, such as two-pass, three-pass and four-pass D-InSAR (Atlantis, 2002). This paper uses four-pass D-InSAR technique with a DEM generated by a pair of C-band SAR images and a pair of L-band SAR images to monitor the location and the magnitude of ground deformations due to mining activities.

Four-pass D-InSAR requires two pairs of SAR radar images from repeat-pass SAR satellite over the area of interest. One pair is used to generate a DEM which contains the topographic information. The other pair, referred as a targeting pair, is used to identify the possible or

expected ground deformation formed between the two acquisitions. The external DEM is used to remove the topographic phase contributions from the interferogram of the targeting pair, hence the changes of ground surface can be detected (Atlantis, 2002; Tsay and Lu, 2001).

A high quality geocoded DEM is generated by a ERS-1 / ERS-2 tandem pair radar images using GPS surveyed ground control points. The details of these two images are listed in Table 1. Note that there is only one day difference between the two acquisitions of the ERS-1/ ERS-2 pair. This small temporal difference gives advantages of high coherence, good height accuracy, and low sensitivity to slow land deformation.

	Satellite	Orbit	Track	Frame	Date yy_mm_dd	Parallel baseline (m)	Perpendicular baseline (m)
Master	ERS1	22434	402	4293	95_10_29	0	0
Slave	ERS2	2761	402	4293	95_10_30	-33	-49

Table 1. The pair of ERS-1/ERS-2 radar image used to generate the external DEM.

The targeting pair is chosen from different combinations of JERS-1 radar images. Even though one cycle of the JERS-1 satellite is 44 days, L-band radar has much less sensitivity to small backscattering changes comparing to C-band ERS-1/ERS-2 radar as the nature of longer wavelength in L-band. As a result, high coherence between two L-band images can still be obtained after 44 days or sometimes even after 132 days, as shown in this paper.

2.1 Generation of D-InSAR results

The first step of four-pass D-InSAR is to generate a high quality DEM which gives the topographic information of the selected scene. The DEM generated by the pair of Table 1 ERS-1/ERS-2 tandem radar image is shown in Figure 1. This DEM will be further used to remove the topographic pattern from the targeting pair of JERS-1 radar images.

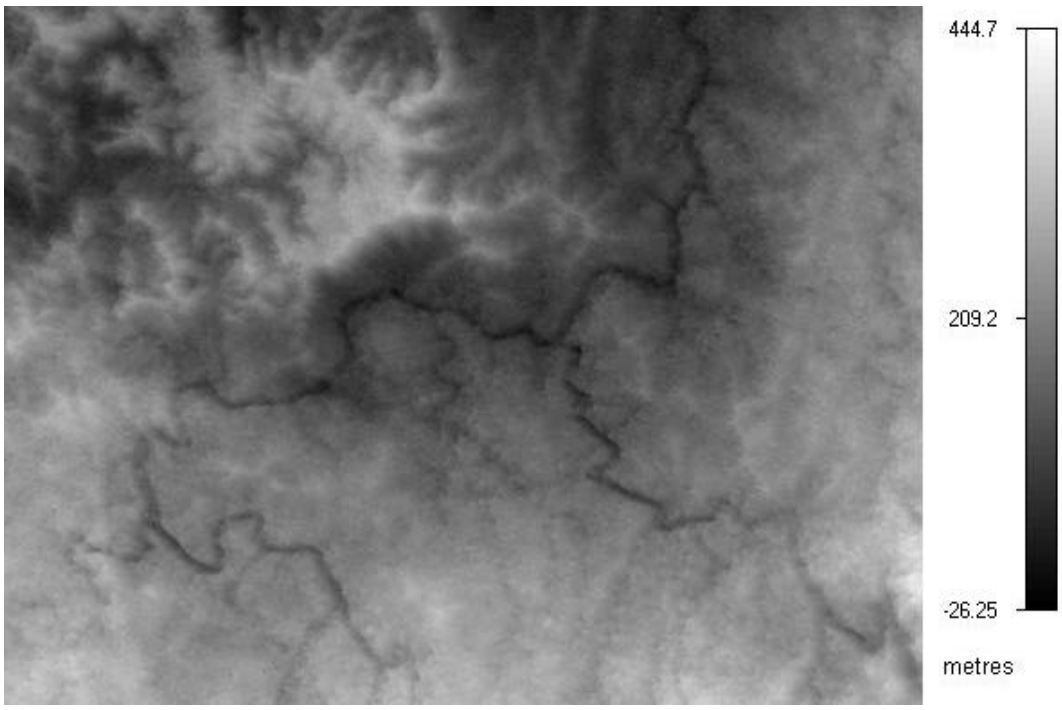

Figure 1. DEM generated from ERS-1/ERS-2 radar images.

The second step is to generate the differential result by using a pair of JERS-1 radar images and the DEM shown in Figure 1. In the EV-InSAR program, the computation steps of generating differential result are coregistration, interferogram generation and finally phase unwrapping and generation of D-InSAR result from the phase (Atlantis, 2002). These steps will be briefly explained in next sections.

Coregistration

This step has two major functions: Firstly, it validates the input master/slave interferometric pair for spatial and spectral overlap. Secondly, it coregisters the DEM and slave SAR image with master image pixel-by-pixel. Therefore, phase difference of each pixel between two SAR images and interferogram can be generated in the next step of Interferogram Generation.

A high quality coregistration can be achieved by having sufficient tie-points, which is normally hundreds. Sometimes, the number of tie-points automatically generated by the EV-InSAR program is insufficient then extra tie-points have to be identified and inputted manually which is very time consuming. A tool, Overlay Tie-pointing Method (OTM), developed by our Satellite Navigation And Positioning (SNAP) research group is used to identify and generate the tie-points automatically. The result is shown in Figure 2.

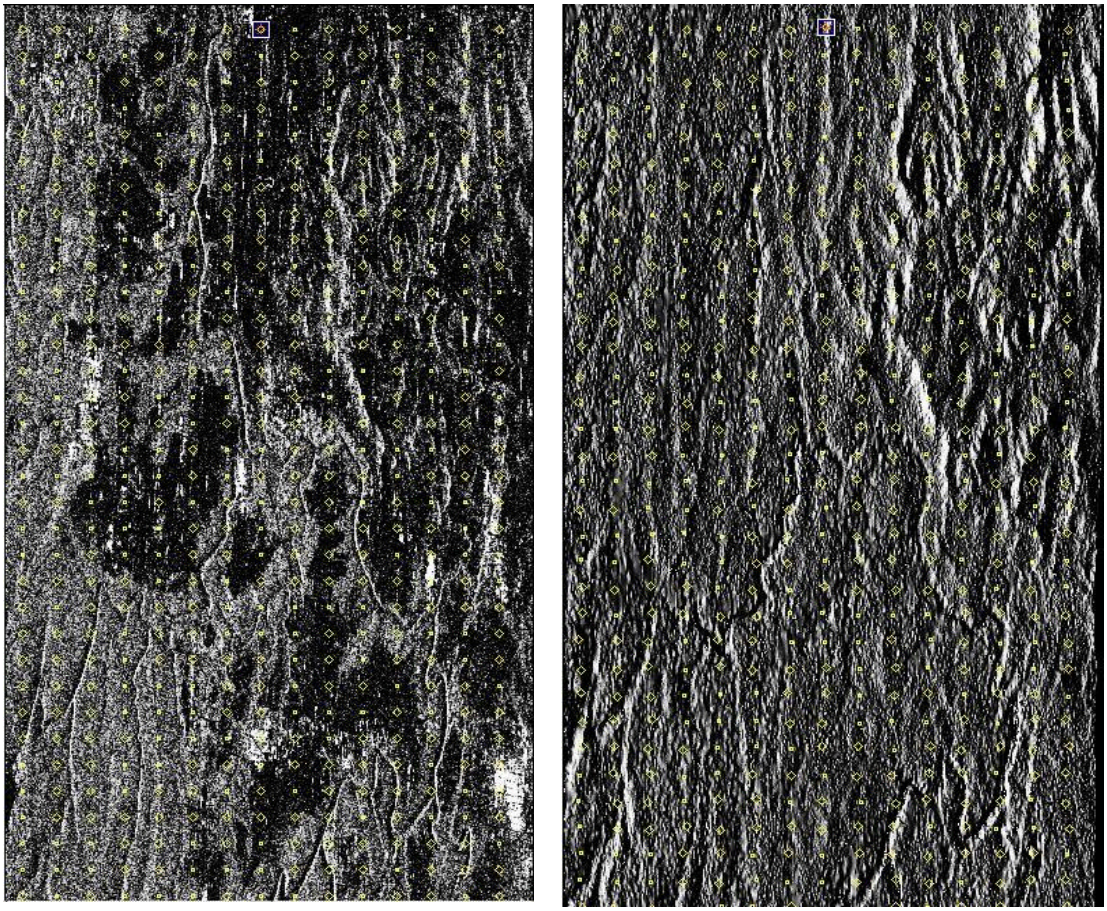

(a) Master image of JERS-1 pair. (b) Simulated SAR image from DEM

Figure 2. The tie-points generated by OTM.

Figure 2 shows the 540 points in total generated by OTM. Each of the small circles indicates the location of successfully refined tie-points and each of the rhombus is the point failed in refinement and therefore being excluded.

Interferogram Generation
The main function of this step is to generate the interferogram and also to filter baseline decorrelation in range, and azimuth spectral overlap in azimuth direction along the way. The residual phase can be also removed manually from the interferogram during this process. A phase coherence map and an unwrapping control mask are generated during the process and can be further used in the next phase unwrapping process.

Phase Unwrapping and Generation of Result
Enhanced interferogram is unwrapped by applying unwrapping control mask. Finally, the estimated D-InSAR height change image is generated.

2.2 D-InSAR Test Results of JESR-1 SAR Radar Images

Different combinations of master/slave pair from JERS-1 radar images have been tested. In this paper, four pairs of JERS-1 data are presented and the details are listed in Table 2.

Pair	Master Image (yyyy_mm_dd)	Slave Image (yyyy_mm_dd)	Perpendicular Baseline (m)	Parallel Baseline (m)	Temporal Baseline (day)
1	1993_11_09	1994_03_21	271.8	160.53	132
2	1995_03_08	1995_04_21	94.11	406.47	44
3	1995_04_21	1995_06_04	482.21	-603.96	44
4	1995_03_08	1995_06_04	557.46	-196.49	88

Table 2. The testing master/slave pairs of JERS-1 radar data.

The differential result of each master/slave pair indicates the magnitude of the ground deformation during the period between the two acquisitions. For example, the differential result of Pair 1 in Table 2 indicates the ground deformation occurred in the next 132 days after the acquisition of the master image. The D-InSAR results of these pairs are shown in Figure 3 and 4. The white spots show the locations of larger deformation with respect to other relatively small or zero ground height change area with darker in grey scale.

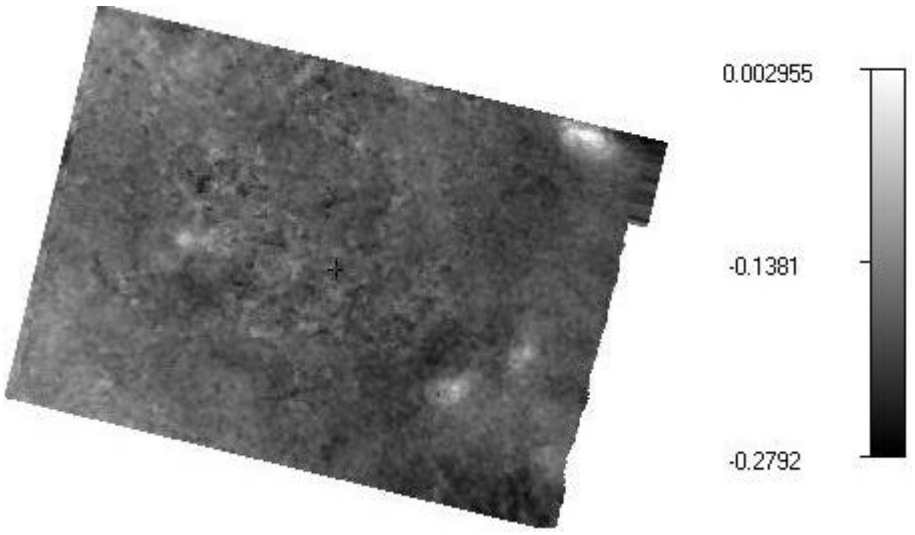

Figure 3. The differential result of Pair 1 in Table 2.

Note that Figure 3 shows the master/slave pair of JERS-1 SAR radar images can still provide sufficient correlation to generate a high quality differential interferometry SAR result even the time difference between the two acquisitions is 132 days.

The scale bars in these differential results indicate the relative height change between the master and slave JERS-1 radar images in metres. The expected ground deformation within a period of 1 ~ 3 cycles is about 20 ~ 30 centimetres. The result in Figure 3 shows the highest quality of these four pairs as its range of relative height change is about 29 centimetres which is similar to the expected value. Also the most of topographic information had been removed from the result in Figure 3 when it can still be seen in the results shown in Figure 4.

The subsidence in Figure 4 (c) is not clearly visible, however, the locations of subsidence can still be identified later on by with the assistance of GIS technique. The combination of D-InSAR and GIS techniques are described in the next section.

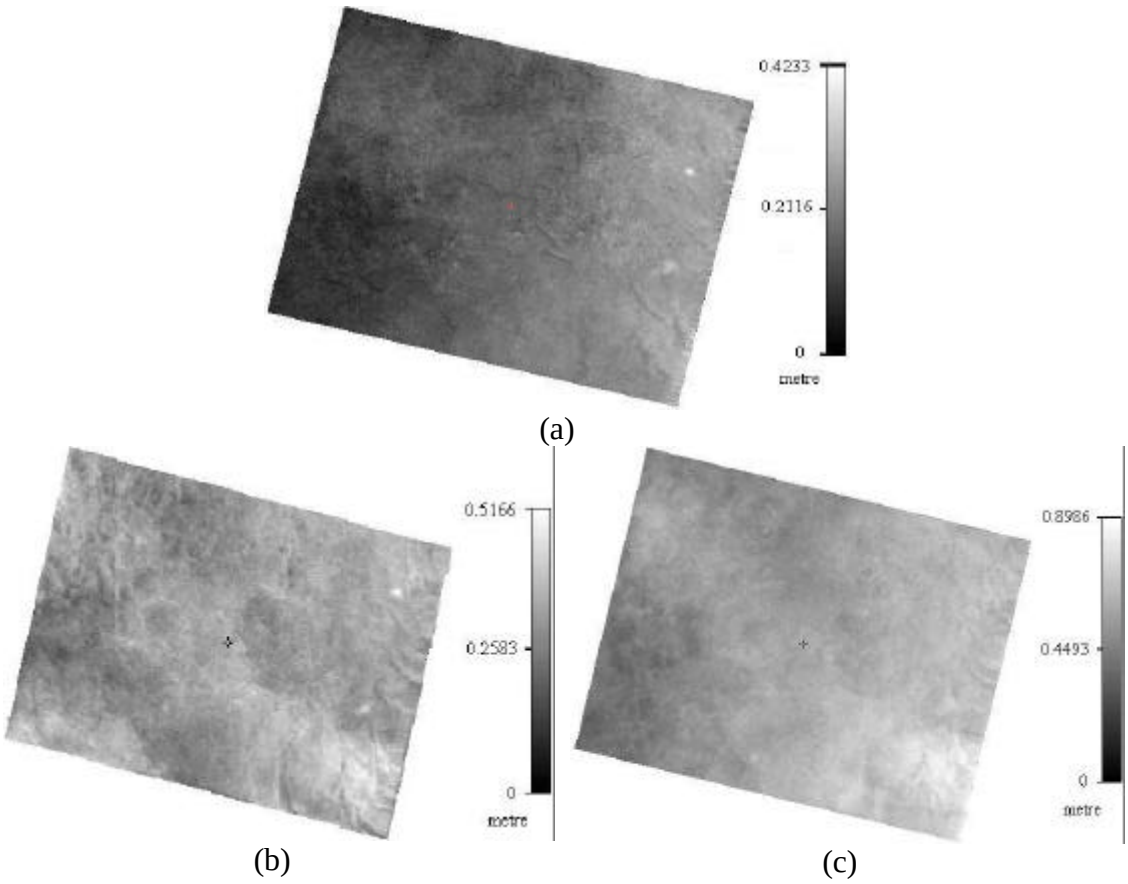

Figure 4. The D-InSAR height change results of (a) Pair 2, (b) Pair 3 and (c) Pair 4 in Table 2.

2.3 Analysis of D-InSAR results

The selected scene is the coverage of underground coal mining sites owned by BHP Billiton. The ground deformations detected by D-InSAR are, therefore, expected to be the consequence of the mining activity. The geocoded height change generated from D-InSAR contains both ground deformation and geographic locations. In this paper, GIS is used to assist the interpretation of D-InSAR results. The GIS software used here is ArcGIS 8.1, a product of ESRI (ESRI, 2003). Figure 5 shows an aerial photo taken over the mining sites, the layout of mine plan and a ground measurement levelling line provided by the BHP Billiton.

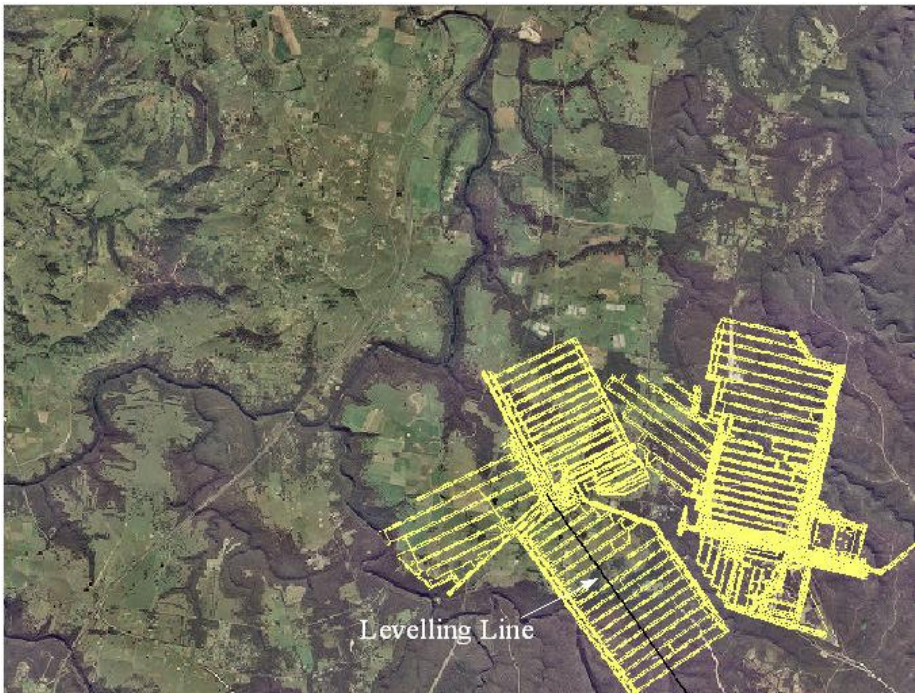

Figure 5. Aerial photo, a ground measurement levelling line and layout of mine plan in Appin and Westcliff, New South Wales, Australia.

The steps of combining the D-InSAR height change results with GIS are georeferencing, reclassifying and masking. These steps are discussed in details in following sections.

Georeference
Georeference is the process to superimpose the D-InSAR height change result to the aerial photo image. Therefore, the location of the subsidence associated to the mining activity during that particular period can be seen clearly on the aerial photo.

Reclassify
The bright spots in the D-InSAR result indicate where the elevation of ground surface has changed the most. These spots are classified as where the subsidences occur. The height change image has to be reclassified so that the subsidence area can be extracted and used for further interpretation.

Mask
After the reclassifying process, there is still some background noise remaining. A masking process is utilised to filter out the unwanted noise and only the subsidence within the mining site will be kept. This is because only the subsidence due to mining activity is of interest here.

The final results after combining D-InSAR and GIS are shown in the Figure 6. These locations of subsidence during the specific periods have been validated with the schedule of mine plan provided by BHP Billiton. Such subsidence data can be archived and delivered easily using GIS.

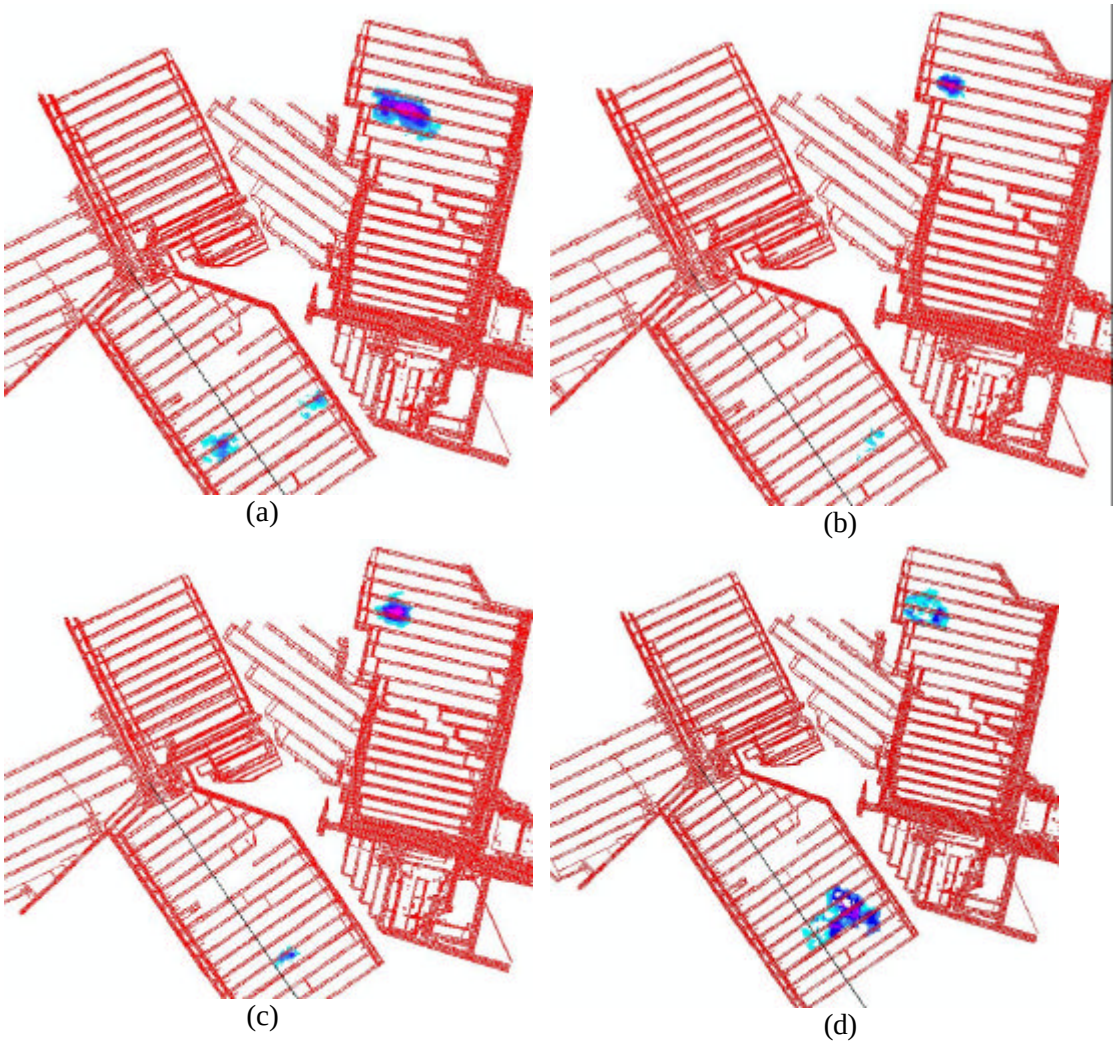

Figure 6. The results of estimated subsidence of Pair 1 ~ 4 in Table 2 after using GIS technique are shown respectively in (a), (b), (c) and (d).

Figure 6 (a) to (d) show the locations of subsidence caused by mining activities during the corresponding periods. The ground deformation should move along the longwall sequentially according to mining direction. This is demonstrated clearly by Figure 6 (b) and (c) where the subsidence at the lower mining site shifted along the same longwall from right to left sequentially. Figure 6 (d) was expected to show only the areas as the summation of the subsidence areas in (b) and (c). However, the correlation in (d) is degraded by possibly poor baselines and perhaps other interference such as tropospheric effect. As a result, the subsidence detected in Figure 6 (d) has both greater coverage areas and magnitude.

As an advantage of applying GIS, ground deformation profiles can be generated along any line across the subsidence area. The profiles of subsidence in Westcliff of Pair 1 are shown in Figure 7. These profiles are plotted along the selected major axis X and minor axis Y of the subsidence basin. These profiles can be used to compare with ground survey data in order to verify the D-InSAR results.

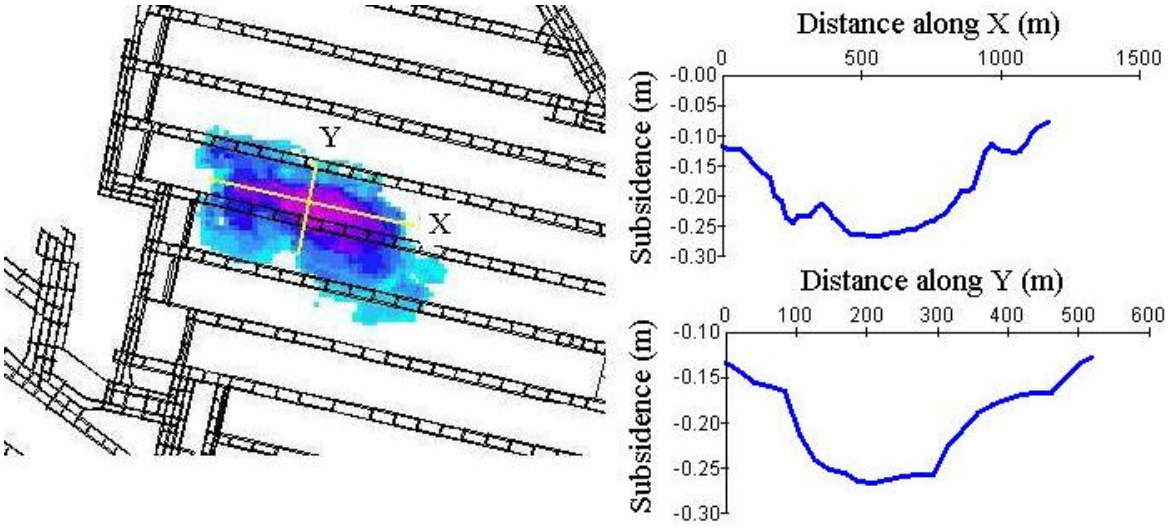

Figure 7. Subsidence profiles derived from Pair 1 (931109 – 940321) JERS-1 DInSAR result for Westcliff.

3. Possible Error Factors

In order to obtain a good correlation between the two radar images, there are some limitations both temporal and spatial (Atlantis, 2002; Mendes et al, 1995):

Temporal decorrelation caused by rainfall, vegetation growth or random motion during the period of the two passes have effects on phase correlation, and hence the quality of the interferogram.

There is also a limit for the baseline separation. The usable perpendicular baseline separation can be up to several hundred metres for ERS-1/2 radar and one to two kilometres for JERS-1.

Last but not least, the earth atmosphere has influence on the propagation of radar waves. The atmospheric conditions vary with changes in height, geographical location and time. A localised model of troposphere effects estimated from GPS observations is therefore essential to correct the interference from atmosphere.

4. Further Work

The next step will be validating our D-InSAR results by comparing with other ground survey data. The ground survey data is sampled along the levelling lines and owned by BHP Billiton. Up until the paper has been published, the requested data has not yet been received by the research team. Several levelling lines are distributed at various mining sites, and the results can only be validated when the subsidence estimated by D-InSAR and the levelling lines are overlapping. This constraint drives the generation of further D-InSAR results.

5. Concluding remarks

Four differential InSAR results derived from the JERS-1 data have been analysed with the help of GPS and GIS. It has been demonstrated in this paper that D-InSAR technique and radar remote sensing in general can be used to detect small ground deformation over a large area

during a specific period. It is proposed to use GPS to assist precise georeference and ensure sub-centimetre accuracy of InSAR results and GIS to interpret, archive, and deliver the subsidence data derived from InSAR. Further work has to be done to validate this technique with ground survey in order to apply this to identify both geographic location and height change of ground subsidence.

Acknowledgment

The authors wish to thank Mr Andrew Nesbitt of BHP for providing GIS data, A/Prof Makoto Omura of Kochi Women's University, Japan, for providing L-band data, and ACRES (the Australian Centre for Remote Sensing) for providing C-band SAR images. The first author is supported by the Australian Research Council.

References

Atlantis Scientific Inc., 2002. EV-InSAR User Guide, Atlantis Scientific Inc., Canada.

Atlantis, 2003. EarthView InSAR, a software product by ATLANTIS, http://www.atlantis-scientific.com/products_services.html

ESRI, 2003. ArcGIS 8.1, a GIS software package by ESRI, http://www.esri.com /software/arcgis/

Mendes, V.B., J.P. Collins, and R.B. Langley, 1995. The Effect of Tropospheric Propagation Delay Errors in Airborne GPS Precision Positioning, ION GPS-95, *8th International Technical Meeting of the Satellite Division of the Institute of Navigation,* Palm Springs, USA, September.

Nestbitt, A., 2003. Subsidence Monitoring West Cliff Colliery Longwall 5A4, APAS *(Association of Public Authority Surveyors) 2003 Conference,* Wollongong, Australia, 1-4 April.

Schofield, W., 1993. *Engineering Surveying*, Laxton's, Oxford, UK, 554pp.

Tsay, J.R., C.H. Lu, 2001. Quality Analysis On Height Displacement Values Determined By Three-Pass Method And Some Test Results In Urban Area In Taiwan, Proc. ACRS 2001 – *22nd Asian Conference on Remote Sensing,* 5-9 November, Singapore. Vol. 2, pp. 977-982.